Materials Research Innovations

ISSN: 1432-8917 (Print) 1433-075X (Online) Journal homepage: http://www.tandfonline.com/loi/ymri20

Photovoltaic and impedance spectroscopic characteristics of heterojunction of graphene-PEDOT:PSS composite and n-silicon prepared via solution-based process

Sanjay Behura, Hatchinghoi Haokip, Charu Goel, Sasmita Nayak, Pramila Mahala, Rahul Kapadia & Omkar Jani

To cite this article: Sanjay Behura, Hatchinghoi Haokip, Charu Goel, Sasmita Nayak, Pramila Mahala, Rahul Kapadia & Omkar Jani (2016): Photovoltaic and impedance spectroscopic characteristics of heterojunction of graphene-PEDOT:PSS composite and n-silicon prepared via solution-based process, Materials Research Innovations, DOI: 10.1080/14328917.2016.1211477

To link to this article: http://dx.doi.org/10.1080/14328917.2016.1211477

Published online: 02 Aug 2016.

Photovoltaic and impedance spectroscopic characteristics of heterojunction of graphene-PEDOT:PSS composite and n-silicon prepared via solution-based process

Sanjay Behura[1*,§], Hatchinghoi Haokip[1†], Charu Goel[1†], Sasmita Nayak[1*,§], Pramila Mahala[2], Rahul Kapadia[1] and Omkar Jani[1]

Recent investigations involving nanoscale energy conversion using two-dimensional nanomaterials such as graphene and transition metal dichalcogenides (TMDs) hold promise to mitigate future energy challenges. The heterojunction devices designed by interfacing 2D layers with 3D bulk semiconductors (2D/3D heterojunctions) including graphene/silicon and TMDs/silicon are widely explored for the photovoltaic characteristics. Developing a thorough understanding of the interfacial chemistry via impedance spectroscopic analysis will leverage the potential of these 2D/3D junctions for large-scale integrations. Here, the non-vacuum solution-processed reduced graphene oxide (rGO), poly(3,4-ethylenedioxythiophene):polystyrene sulphonate (PEDOT:PSS) and their composite (PEDOT:PSS(rGO)) were spin coated on the silicon (n-Si) substrates for fabrication of heterojunctions, with the device construct of rGO/n-Si, PEDOT:PSS/n-Si and PEDOT:PSS(rGO)/n-Si having Ohmic metal contacts in both top and bottom. The significant efficiency improvement of three orders for PEDOT:PSS(rGO)/n-Si device over the rGO/n-Si and PEDOT:PSS/n-Si heterojunction devices can be attributed to (i) increased conducting channels in the active region and (ii) reduced series resistance. Further, the impedance spectroscopy is employed to understand the interfacial chemistry of PEDOT:PSS(rGO)/n-Si solid-state junction, which is explained by a parallel resistance–capacitance circuit model.

Keywords: Nanostructure, Chemical synthesis, Impedance spectroscopy, Electrical properties, Solar cells, Composites, Graphene, Conducting polymer

Introduction

The renewable energy research and development is of prime importance for the present time and in order to achieve the grid parity for solar energy, the worldwide photovoltaic researchers are constantly exploring innovative materials for the design of solar cells to reduce cost and boost efficiency. The silicon (Si) wafer-based homojunction (p-Si/n-Si) solar cell technology is expensive and further the efficiency is capped via Shockley–Queisser limit.[1] Alternatively, interfacing two-dimensional (2D) layers and three-dimensional (3D) bulk semiconductors (2D/3D heterojunction) holds promise for cost-effective and efficient nanoscale energy conversion.[2] In this context, the atomically thin 2D nanomaterials such as graphene and transition metal dichalcogenides (MoS_2 or WS_2, etc.) have been leveraged due to their exotic properties suitable for optoelectronics.[3] Further, the reduced graphene oxide (rGO) produced via chemical exfoliation method[4] possess excellent features of mass production and can be integrated into novel device applications.[5] Recently, rGO/Si interface has been probed as a potential photovoltaic device for fundamental understanding and large-scale applications.[3b] It is important to note that the rGO/Si device construct is advantageous over various 3D/3D semiconductor junctions because: (i) first, the top graphene layer is both transparent and conducting, therefore can be used as transparent current-spreading electrode[6] and (ii) second, it can act as active solar cell layer with controlled synthesis methods.[7]

Further, the combination of rGO and poly(3,4-ethylenedioxythiophene):polystyrene sulphonate (PEDOT:PSS) is attractive and has shown excellent performance in optoelectronic device applications.[8] The combination of rGO and PEDOT:PSS is believed to enhance the device performance owing to their enhanced optical, mechanical and electrical properties. The present work demonstrates the design, fabrication and photovoltaic characterisations of heterojunctions made from rGO and PEDOT:PSS with n-Si. Furthermore, a thorough impedance spectroscopic analysis is carried out on PEDOT:PSS(rGO)-on-Si solid-state junction considering its superior performance.

[1]Solar Energy Research Wing, Gujarat Energy Research and Management Institute – Research, Innovation and Incubation Centre, Gandhinagar 382007, Gujarat, India
[2]Department of Solar Energy, Pandit Deendayal Petroleum University, Gandhinagar 382007, Gujarat, India

*Corresponding authors, emails sbehura1@uic.edu, sanjaybehura@gmail.com (Sanjay Behura); sasmita.nayak11@gmail.com (Sasmita Nayak)
†Both the authors have contributed equally.
§Present address: Department of Chemical Engineering, University of Illinois at Chicago, 810 S. Clinton Street, Chicago, IL 60607, USA

Received 8 May 2016; accepted 4 July 2016
DOI 10.1080/14328917.2016.1211477

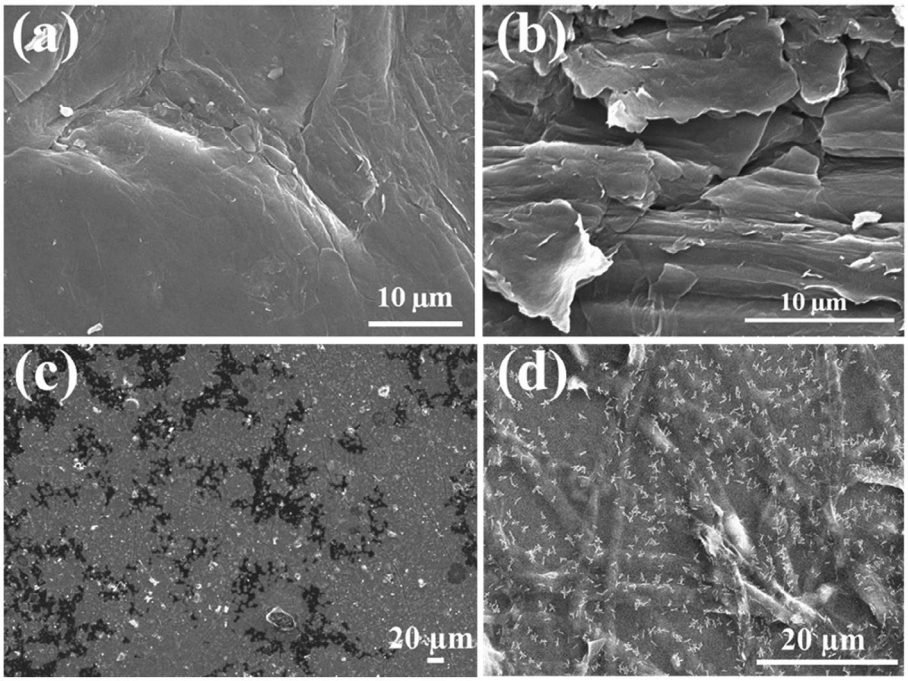

1 SEM micrographs of *a* GO, *b* rGO, *c* PEDOT:PSS and *d* PEDOT:PSS(rGO) composite

Experimental

The graphene oxide (GO) was prepared via modified Hummers' method[9] and further chemically reduced to rGO via a strong reducing agent ($NaBH_4$). For the reduction process, the GO of 0.7566 g was dispersed in 20 ml of 1 M freshly prepared aqueous $NaBH_4$ solution under vigorous stirring for 10 min and finally the rGO powder was collected by filtration. Further, 0.5 ml of PEDOT:PSS solution was mixed with 5 ml of 0.1 wt% rGO for preparation of the composite of rGO and PEDOT:PSS suspension.[7] Finally, the solution-processed rGO, PEDOT:PSS and their composite (PEDOT:PSS(rGO)) were spin coated on the pre-treated silicon (n-Si) substrates for fabrication of heterojunctions, with the device construct of rGO/n-Si, PEDOT:PSS/n-Si and PEDOT:PSS(rGO)/n-Si. The spin coating was performed at a rotation speed of 500 rpm for 60 s and the post-spin coated samples were further baked at 80 °C for 10 min.

Results and discussion

Structural characteristics

The scanning electron microscopy (SEM) micrographs of GO, rGO, PEDOT:PSS and PEDOT:PSS(rGO) composite structures are shown in Fig. 1*a–d*, respectively. The GO exhibits high surface area, shiny and smooth morphology which indicates proper exfoliation of graphite during chemical oxidation process. The rGO possesses flaky structures with flake size about 10 μm and flakes are overlapping to form a compact structure. The PEDOT:PSS layer is uniform on the substrate with lateral dimensions ranging from 10 to 50 μm. The surface morphology of PEDOT:PSS(rGO) resembles strongly folded decoration of rGO on which PEDOT:PSS nanoparticles are deposited uniformly, which further indicates that rGO flakes are overlapped rather than aggregated with particle-like mixed composite structure reflecting the platelet homogeneity. The detailed Raman spectroscopic characterisations of GO, rGO and PEDOT:PSS(rGO) were mentioned in our earlier report.[3b, 7]

Photovoltaic characteristics

To investigate the potential application of rGO and PEDOT:PSS in photovoltaic devices, rGO/n-Si, PEDOT:PSS/n-Si and PEDOT:PSS(rGO)/n-Si heterojunctions were fabricated via the process as mentioned in the experimental section. Figure 2*a* and *b* shows the schematic of PEDOT:PSS/n-Si, rGO/n-Si and composite PEDOT:PSS(rGO)/n-Si heterojunction solar cell devices and the corresponding generalised band diagram at equilibrium conditions, respectively. The photovoltaic devices were analysed by current density–applied voltage (J–V) characterisation under dark and AM 1.5G (100 mW/cm^2) light illuminations. The device parameters (reverse saturation current (J_o) and barrier height (ϕ_B)) and photovoltaic parameters (short circuit current density (J_{sc}), open circuit voltage (V_{oc}), fill factor (FF), efficiency (η), series resistance (R_s) and shunt resistance (R_{sh})) are calculated from Fig. 3 and summarised in Table 1.

The current–voltage characteristics for a Schottky barrier diode with assumption that the current is due to thermionic emission can be expressed as: $J = J_o\,[\exp(V_D/nk_BT)-1]$, where J is the diode current, J_o is the reverse bias saturation current, V_D is the voltage across the diode, k_BT is the thermal voltage, (k_B is the Boltzmann constant and T is the temperature in Kelvin) and n is the ideality factor (which are derived from the slope of Ln (J)–V curve). J_o can be extracted by extrapolating the straight line of Ln (J) to intercept the axis at zero voltage: $J_o = AA^*T^2 \exp(-q\Phi_B/k_BT)$, where A is the effective area of the device (1 cm^2), A^* is the Richardson constant. The Schottky barrier height for three representative devices are calculated following the formula: $\Phi_B = k_BT/q\,\ln(AA^*T^2/J_o)$.

Figure 3*a* and *b* depict J–V characteristics for PEDOT:PSS/n-Si device under dark and AM 1.5G illuminations, respectively. Further, the inset of Fig. 3*a* and *b* represents (Ln) J vs. V and the fourth quadrant of J vs. V plot, respectively. Similarly, Fig. 3*c* and *d* show rGO/n-Si device and Fig. 3*e* and *f* present PEDOT:PSS(rGO)/n-Si device under dark and AM 1.5G illuminations. The photovoltaic parameters for PEDOT:PSS/n-Si are (J_{sc} – 0.057 A/m^2, V_{oc} – 0.13 V,

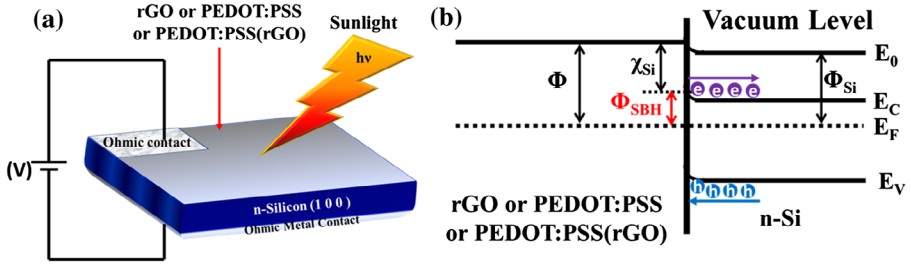

2 The rGO/n-Si, PEDOT:PSS/n-Si and PEDOT:PSS(rGO)/n-Si heterojunctions: *a* schematic of photovoltaic device and *b* band-diagram at equilibrium

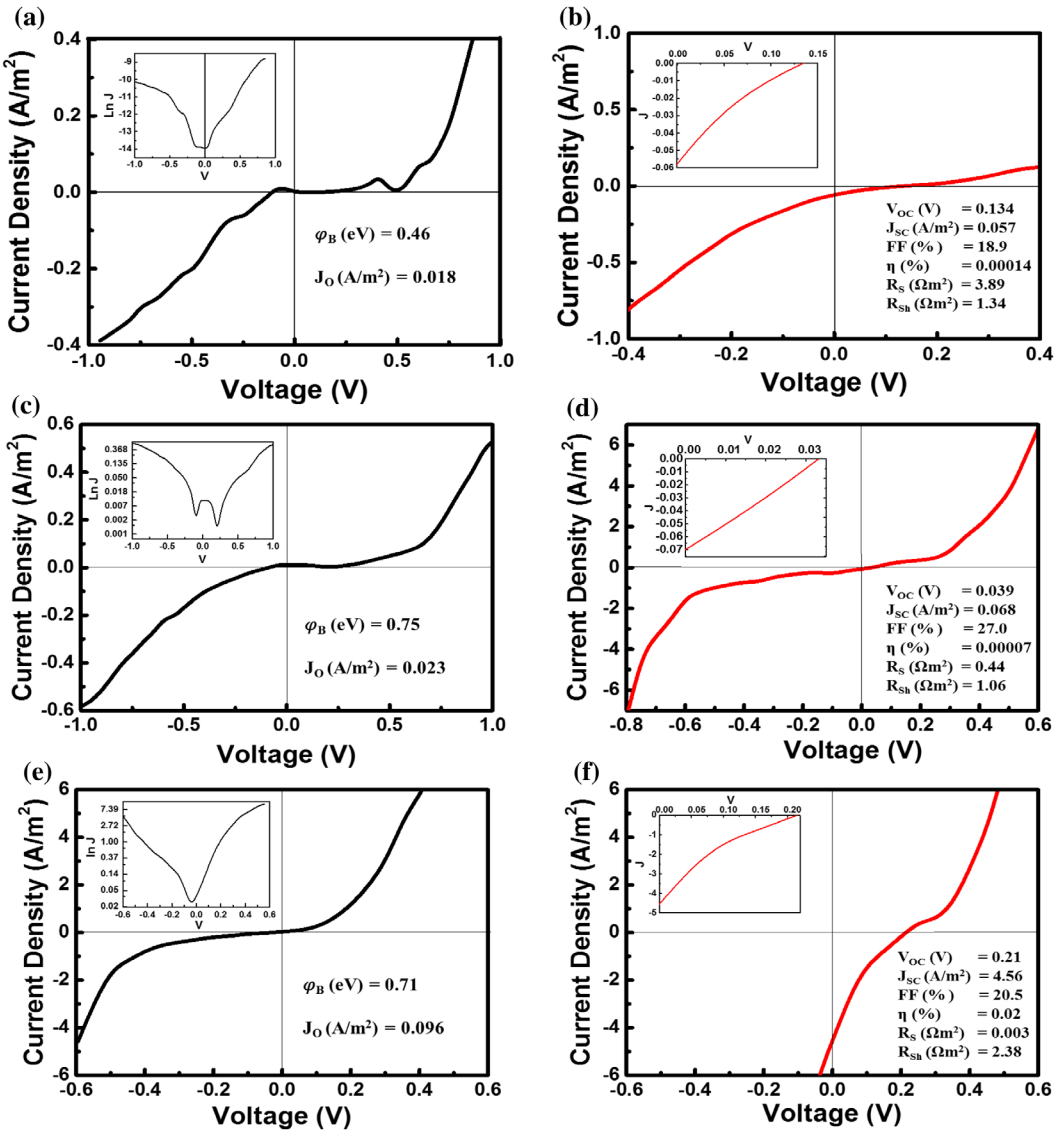

3 Characteristic plot of *J* vs. *V*: for *a* PEDOT:PSS/n-Si under dark and *b* under AM 1.5G illuminations. Insets in *a* is Ln *J* vs. *V* and in *b* is the *J* vs. *V* curve in fourth quadrant, *c* rGO/n-Si under dark and *d* under illuminations. Insets in *c* is Ln *J* vs. *V* and in *d* is the J vs. V curve in fourth quadrant, *e* plot of *J* vs. *V* for PEDOT:PSS(rGO)/n-Si under dark and *f* light. Insets in *e* is Ln *J* vs. *V* and in *f* is the plot *J* vs. *V* curve in fourth quadrant

FF – 18.9%, R_s – 3.89 Ωm², R_{sh} – 1.34 Ωm²), for rGO/n-Si are (J_{sc} – 0.068 A/m², V_{oc} – 0.039 V, FF – 27.0%, R_s – 0.44 Ωm², R_{sh} – 1.06 Ωm²) and for PEDOT:PSS(rGO)/n-Si are (J_{sc} – 4.56 A/m², V_{oc} – 0.21 V, FF – 20.5%, R_s – 0.003 Ωm², R_{sh} – 2.38 Ωm²). The parasitic resistances such as R_s and R_{sh} in the devices are evaluated by plotting the slope in *J*–*V* curve at V_{oc} and J_{sc} point, respectively. It can be noted that in the PEDOT:PSS(rGO)/n-Si solar cell, the R_s is low, i.e. 0.003 Ωm² and consequently, the efficiency is high compared to other devices as it is understood that the critical impact of R_s is to reduce the FF of the device. The efficiency obtained for PEDOT:PSS/n-Si is 0.00014%, for rGO/n-Si is 0.00007% and for PEDOT:PSS(rGO)/n-Si is 0.02%. The efficiency of devices with PEDOT:PSS is higher than the device with

Table 1 Photovoltaic characteristic parameters of three representative heterojunction devices

	Heterojunction devices		
Device parameters	PEDOT:PSS/n-Si	rGO/n-Si	PEDOT:PSS(rGO)/n-Si
J_{SC} (A/m^2)	0.057	0.068	4.56
V_{OC} (V)	0.13	0.040	0.21
FF (%)	18.9	27.0	20.5
η (%)	0.00014	0.00007	0.02
R_s (Ωm^2)	3.89	0.44	0.003
R_{sh} (Ωm^2)	1.34	1.06	2.38

synthesised rGO as expected because of the higher optical transmittance of PEDOT:PSS.[7] The PEDOT:PSS(rGO)/n-Si heterojunction device with composite PEDOT:PSS and rGO exhibits highest efficiency among all the devices. The resulting optimised parameters show increase in cell efficiency from 0.00014% for PEDOT:PSS/n-Si to 0.02% for PEDOT:PSS (rGO)/n-Si device. This improvement in device performance via solution process mixing of PEDOT:PSS with rGO can be attributed to the formation of uniform thin film and conducting channels in the active region. It is also very important to note that, in the composite due to the formation of conducting network, the charge carrier transport is accelerated. Thus, there is improvement in J_{sc} and decrease in R_s compared to rest of the devices due to the uniformity and enhanced conductivity achieved via mixed platelet composite layer. In contrast, efficient solar cell devices based on rGO/Si[10] and PEDOT:PSS/Si[11] heterojunctions are available. In order to improve the efficiency of the heterojunction solar cells presented here, a number of factors can be considered. Those include: (i) efficient light trapping management using plasmonics effect, (ii) back surface doping and (iii) use of proper Ohmic metal front and back contacts, etc.

Impedance spectroscopic analysis

Impedance spectroscopy (IS) is a well-known and widely established technique, which can describe a solid-state device through an equivalent circuit to understand electrical transport phenomena under various conditions.[12] The frequency is an implicit variable in this measurement and varied from 0.1 Hz to 1 MHz. We utilised the IS technique to analyse the solar cells developed here, especially the interfacial chemistry. The IS measurements were performed in a potentiostat/galvanostat (Autolab, model PGSTAT302N) attached with a frequency response analysis module (FRA32M). The measurement for the developed devices was carried out using an AC signal of amplitude 5 mV over the V_{oc} at the frequency range of 0.1 Hz to 1 MHz superimposed by a DC bias of 10 mV under actual dark conditions. The Nyquist, Mott–Schottky (MS) and Bode plots of the impedance spectra for the PEDOT:PSS(rGO)/n-Si heterojunction device are displayed in Fig. 4. The capacitance–voltage (C–V) measurement of the device was conducted at a frequency of 1 kHz to determine the flat-band potential (V_{fb}) and dopant density (N_D) of the device using MS equation,[13]

$$\frac{1}{C^2} = \frac{2}{\varepsilon\varepsilon_0 A^2 q N_D}\left(V - V_{fb} - \frac{kT}{q}\right)$$

where C is the depletion-layer capacitance per unit surface area, N_D is the number of dopant densities, ε_0 is the permittivity of vacuum, ε is the dielectric constant of the semiconductor, V is the electrode potential, V_{fb} is the flat-band potential, k is the Boltzmann constant, T is the absolute temperature and q is the elementary charge. Figure 4*a* presents the MS plot of

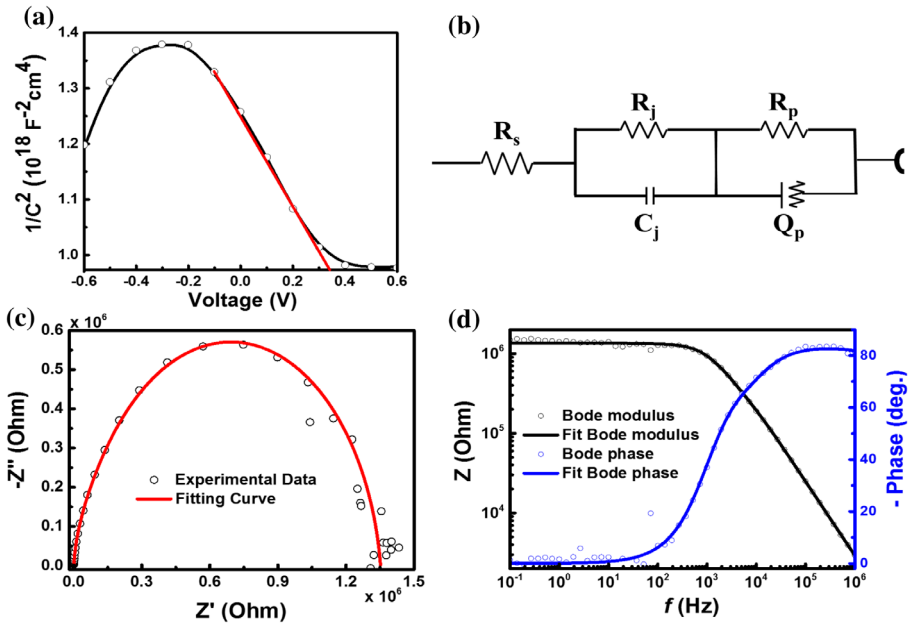

4 Impedance spectroscopy of PEDOT:PSS(rGO)/n-Si heterojunction solar cell: *a* Mott–Schottky (MS) characteristics, *b* equivalent circuit model (R–C) *c* Nyquist plot and *d* Bode plot

Table 2 Estimated fitting parameters of the equivalent circuit for PEDOT:PSS(rGO)/n-Si solar cell from the impedance spectroscopy

		RC-1 circuit		CPE circuit			Time constant	
Device	R_s (Ω)	C1 (pF)	R_1 (Ω)	R_2 (Ω)	Q (pMho)	n	τ (μs)	τ (μs)
PEDOT:PSS (rGO)/n-Si	434	363	46.8 k	1.31 M	235	0.917	0.017	12.14

PEDOT:PSS(rGO)/n-Si heterojunction device. The V_{fb} can be determined from the slope, i.e. drawn in the linear region of the MS plot. From the extrapolation of the MS plot, the V_{fb} for the device is found to be 0.34 V. The N_D determined from the slope for PEDOT:PSS(rGO)/n-Si device is found to be 2.48×10^{18} cm^{-3}.

The AC impedance of a given circuit including resistive and reactive elements at an angular frequency ω is nominally presented as: $Z(\omega) = Z'(\omega) - jZ''(\omega)$, where Z' and Z'' are the real and imaginary parts of the impedance, respectively. Usually the data resemble the shape of an arc of a circle with the centre on or below the axis of Z'. The data can be modelled with one simple parallel resistance–capacitance (R–C) circuit with a resistor (R_j) and a capacitor (C_j) connected in parallel as shown in Fig. 4*b*. The R_j is associated with the material layer resistance and C_j is related to geometric capacitance of the layer PEDOT:PSS(rGO) and n-Si. However, due to the mismatch between the Fermi level of the contact electrode and polymer material, a contact resistance is usually present in all practical devices.[14] Therefore, a series resistance (R_s) is considered in addition to R_j and C_j, when the data are simulated. When the experimental curve was fitted to the R–C circuit, a fine fit was not obtained. Further, we found that such a depressed circular arc can be more appropriately modelled by replacing the capacitor by a constant-phase element (CPE).[15] The CPE has the impedance in the form of

$$Z_{CPE} = \frac{1}{(j\omega)^n Q}$$

where Q is a constant and n is the exponent with a value between $0 < n < 1$. The exponent n describes the degree of capacitive nature of the component, for the ideal capacitor (the n ranges from 0.9 to 1.0).

To fit our experimental results, we need one R–C and one R–Q network in the equivalent circuit, where both R_j parallel to C_j, R_p parallel to Q_p, and series to R_s (Fig. 4*b*). In the present case, the total impedance can be written as

$$Z(\omega) = R_s + \frac{1}{\frac{1}{R_j} + \frac{1}{C_j}} + \frac{1}{\frac{1}{R_p} + \frac{1}{Z_{CPE_p}}}$$

where R_s is the total series resistance due to probe and electrode contacts. Here, the (R_j, C_j) and (R_p, Q_p) are the parallel resistance and CPE impedance pair of p-n junction and back contact, respectively. The incorporation of CPE in the circuit system has been generally estimated to characterise non-ideal capacitance. Previously proposed physical arguments on CPE comprise distribution of energy states, spatially distributed conductivity, dispersive (frequency-dependent) dielectric property, etc.[16] Hence, the observation of a CPE in our result from the PEDOT:PSS(rGO)/n-Si device can most probably be attributed to the inhomogeneous contact interface between the PEDOT:PSS(rGO) surface and the metal electrodes. The low-frequency region (0.1 mHz–1 kHz) represents the material layer resistance (R_j) and the high-frequency region (1 kHz–1 MHz) corresponds to CPE impedance as shown in Bode plot (Fig. 4*d*). The IS data obtained by fitting the impedance spectra of PEDOT:PSS(rGO)/n-Si device are presented in Table 2.

Conclusions

In summary, we have demonstrated the design of solid-state heterojunction devices such as: rGO/n-Si, PEDOT:PSS/n-Si and PEDOT:PSS(rGO)/n-Si produced via non-vacuum solution-based processes. The fabrication technique presented here can be exploited for other applications replacing high-cost procedures. Out of all the heterojunction solar cells, the PEDOT:PSS(rGO)/n-Si structure showed higher efficiency of 0.02%, which can be attributed to (i) formation of increased conducting channels in the active region of the device and (ii) lower series resistance of the device. The impedance spectroscopic data are well fitted by an equivalent circuit containing a CPE that accommodates the non-ideal capacitor due to geometrical inhomogeneity. Thus, it is believed that these results will provide new insight for solar cell researcher to manipulate rGO and conducting polymers. Futuristically, the interfacial science presented here can be extended to further understand via atomistic simulations in order to achieve efficient nanoscale energy conversion.

Acknowledgements

S.B. is thankful to Gujarat Energy Research and Management Institute, Gandhinagar and Pandit Deendayal Petroleum University, Gandhinagar, Gujarat, India for the support to complete this research work. H.H. and C.G. wish to thank Prof. T. Harinarayana, Director-GERMI for the internship opportunity under 'GERMI Summer Internship Programme 2014'.

Funding

This work was supported by the Gujarat Energy Research and Management Institute.

References

1. W. Shockley and H. J. Queisser: *J. Appl. Phys.*, 1961, **32**, (3), 510–519.
2. B. Li, G. Shi, S. Lei, Y. He, W. Gao, Y. Gong, G. Ye, W. Zhou, K. Keyshar, J. Hao, P. Dong, L. Ge, J. Lou, J. Kono, R. Vajtai and P. M. Ajayan: *Nano Lett.*, 2015, **15**, (9), 5919–5925.
3. (a)L. Britnell, R. M. Ribeiro, A. Eckmann, R. Jalil, B. D. Belle, A. Mishchenko, Y.-J. Kim, R. V. Gorbachev, T. Georgiou, S. V. Morozov, A. N. Grigorenko, A. K. Geim, C. Casiraghi, A. H. C. Neto and K. S. Novoselov: *Science*, 2013, **340**, (6138), 1311–1314.(b)S. K. Behura, S. Nayak, I. Mukhopadhyay and O. Jani: *Carbon*, 2014, **67**, 766–774. (c)S. Behura and V. Berry: *ACS Nano*, 2015, **9**, (3), 2227–2230.
4. S. Pei and H.-M. Cheng: *Carbon*, 2012, **50**, (9), 3210–3228.
5. X. Xu, D. Huang, K. Cao, M. Wang, S. M. Zakeeruddin and M. Grätzel: *Sci. Rep.*, 2013, **3**, 1489-1–1489-7.
6. (a)S. K. Behura, P. Mahala, S. Nayak and O. Jani: *AIP Adv.*, 2014, **4**, (11), 11711-1–11711-5.(b)Y. Xu and J. Liu: *Small*, 2016, **12**, (11), 1400–1419.
7. P. Mahala, A. Kumar, S. Nayak, S. Behura, C. Dhanavantri and O. Jani: *Superlattices Microstruct.*, 2016, **92**, 366–373.
8. D. W. Chang, H.-J. Choi, A. Filer and J.-B. Baek: *J. Mater. Chem. A*, 2014, **2**, (31), 12136–12149.

9. W. S. Hummers and R. E. Offeman: *J. Am. Chem. Soc.*, 1958, **80**, (6), 1339–1339.
10. G. Kalita, K. Wakita, M. Umeno and M. Tanemura: *Physica status solidi (RRL) – Rapid Res. Lett.*, 2013, **7**, (5), 340–343.
11. K. A. Nagamatsu, S. Avasthi, J. Jhaveri and J. C. Sturm: *IEEE J. Photovoltaics*, 2014, **4**, (1), 260–264.
12. J. R. Macdonald and W. B. Johnson: 'Fundamentals of impedance spectroscopy', in 'Impedance spectroscopy', (ed. E. Barsoukov and J. Ross Macdonald), 1–26; 2005, John Wiley & Sons.
13. K. Gelderman, L. Lee and S. W. Donne: *J. Chem. Educ.*, 2007, **84**, (4), 685–688.
14. A. Kumatani, Y. Li, P. Darmawan, T. Minari and K. Tsukagoshi: *Sci. Rep.*, 2013, **3**, 1026-1–1026-6.
15. J. Ross Macdonald: *Solid State Ionics*, 1984, **13**, (2), 147–149.
16. (a)C.-C. Chen, B.-C. Huang, M.-S. Lin, Y.-J. Lu, T.-Y. Cho, C.-H. Chang, K.-C. Tien, S.-H. Liu, T.-H. Ke and C.-C. Wu: *Org. Electron.*, 2010, **11**, (12), 1901–1908.(b)J. Drechsel, B. Männig, D. Gebeyehu, M. Pfeiffer, K. Leo and H. Hoppe: *Org. Electron.*, 2004, **5**, (4), 175–186.